CrystEngComm

Accepted Manuscript

ROYAL SOCIETY OF CHEMISTRY

www.rsc.org/crystengcomm

Journal Name

ARTICLE

Metal(II)–Organic frameworks with 3,3′--diphenyldicarboxylate and 1,3-bis(4-pyridyl)propane: preparation, crystal structures and luminescent properties

Received 00th January 20xx,
Accepted 00th January 20xx

DOI: 10.1039/x0xx00000x

www.rsc.org/

Ting-Ting Fan, Jia-Jia Li, Xiang-Long Qu, Hong-Liang Han, Xia Li*

Mixing transition metal (II) salts with a 3,3′-diphenyldicarboxylic acid (3,3′-H_2dpdc) and 1,3-bis(4-pyridyl)propane (bpp) led to the complexes, [M(3,3′-dpdc)bpp] (M= Zn **1**, Cd **2**) and [Cu_2(3,3′-dpdc)$_2$(bpp)] (**3**). These complexes were characterized by single crystal X-ray diffraction. **1** possesses a four fold-interpenetrating 3D diamondoid framework consisting of Zn-3,3′-dpdc and Zn-3,3′-dpdc-bpp helices and has 6^6 topology net with 4-c tetrahedral Zn(II) nodes. **2** exhibits a 3D framework consisting of Cd-3,3′-dpdc-bpp two/four--stranded helices and has 6-c {$3^6.4^{12}.5^4.6^6$} topology with binuclear blocks. **3** ha three fold-interpenetrating 3D framework with 6-c {$3^{12}.4^{28}.5^5$} topology based on binuclear blocks. Cu-3,3′-dpdc and Cu-bpp-3,3′-dpdc helices are formed. The metal centers play a crucial role in the system structure direction. The luminescent properties of those compounds were investigated. The results show that **1** can be used as a fluorescence probe to detect benzaldehyde and sensitize Tb(III) luminescence. Notably, addition of Tb(III) into the Zn-MOF (**1**) greatly enhanced ti ability to detect benzaldehyde

Introduction

The metal-organic frameworks (MOFs) attract more and more attention due to their intriguing architectures and their potential properties in separation, ion exchange, catalysis, sensors, magnetism and gas storage.[1] Recently, MOFs were also designed as fluorescence probes to detect materials such as dyes, rare-earth metal ions and explosive molecules.[2] Such probes have important applications in biological and environmental systems. Numerous metal-organic frameworks containing different types of entanglements networks have been reported. In particular, the microporous and interpenetrating network structures are extensively explored in crystal engineering of coordination polymer because these compounds have attractive topologies, intriguing structural features and properties, and might be used to selectively adsorb and separate some materials.[3] Such coordination frameworks can be constructed by combining organic ligands 'spacers' with metal 'nodes'.[4]Transition metal cations have a variety of coordination geometry, and can be used in a variety of crystal architectures through the imposition of their coordination environment. Furthermore, transition metal- based MOFs are potential materials in optical applications, such as fluorescence probes and nonlinear optical materials.[1f-h] The carboxylate group is a well-known ligand that can bridge metal centers to form multitudinous frameworks through different bridging modes. Semi-rigid polycarboxylic acids usually contain aromatic carboxylic acid moieties, which are widely used as linkers in coordination polymers.[5] Because they have both rigid and flexible moieties, such acids may be used to develop novel coordination polymers with helical and interpenetrating structures. Conformational flexible N-ligands are proven to be useful in constructing intriguing self-penetrated networks. It is reported that flexible N-based bridgi ligands could be successfully utilized to prepare coordination polymers with fascinating topologies and interpenetrating network structures.[6,7] Therefore, the combination of carboxylic acids and N-ligands as spacers would be a better strategy to synthesize MOFs.[5-7] We are interested in the design, synthesis and characterization of transition metal- based MOFs, and want to develop MOFs-based luminescent probes for ions or organic molecules detection. In this work, we investigated the transition metal (II) coordination polymers with 3,3′-diphenyldicarboxylic acid (3,3′-H_2dpdc) and flexible 1,3-bis(4-pyridyl)propane (bpp) as ligands. 3,3′-H_2dpdc, a long and semi-rigid ligand composed of two aromatic carboxylic acid moieties, can freely twist its benzene rings to meet the requirements of the coordination geometries of metal ions during the assembly process. However, the semi-rigid 3,3′-H_2dpdc was rarely used in MOFs.[8] The bpp is a long and flexible building block and can adopt different conformations (TT, TG, GG and GG′) (Scheme S1[7a]) depending on the relative orientations of the three CH_2 groups between two pyridine rings.[7] A combination of the two types of ligands may yield novel microporous compounds with helical or interpenetrating network. Thus, three new coordination polymers, [M(3,3′-dpdc)bpp] (M= Zn **1**, Cd **2**) and [Cu_2(3,3′-dpdc)$_2$(bpp)] (**3**) were hydrothermally synthesized and structurally characterized. These MOFs show remarkable diversities and unique structural features. Complex **1** possesses a four fold-interpenetrating 3D framework with 6^6 topology, **2** exhibits a 3

Beijing Key Latoratory for Optical Materials and Photonic Devices, Department of Chemistry, Capital Normal University, Beijing, 100048, China.
E-mail: xiali@cnu.edu.cn; Fax: +86 10 68902320; Tel: +86 10 68902320
†Electronic Supplementary Information (ESI) available: CCDC: 1402459, 1402456, 1402458. For ESI and crystallographic data in CIF or other electronic format See DOI: 10.1039/x0xx00000x

framework with $\{3^6.4^{12}.5^4.6^6\}$ topology, and **3** has a three fold-interpenetrating 3D framework with $\{3^{12}.4^{28}.5^5\}$ topology. Zn-3,3′-dpdc and Zn-3,3′-dpdc-bpp helices, Cd-3,3′-dpdc-bpp two/four--stranded helices, and Cu-3,3′-dpdc and Cu-bpp-3,3′-dpdc helices are formed in **1-3**, respectively. In addition, our research show that these MOFs have interesting and important fluorescent properties and **1** is very sensitive to benzaldehyde molecule and Tb(III) ion. Herein, the syntheses, crystal structures, and photoluminescence properties of **1**–**3** are reported.

Experimental section

Materials and physical measurements

All reagents were commercially purchased and used without further purification.

Elemental analyses of C, H and N were performed on an Elemental Vario EL analyzer. X-ray diffractionwas carried out on a PANaytical X'Pert PRO MPD diffractometer for Mo Kα radiation (λ = 0.71073 Å), with a scan speed of 2°·min^{-1} and a scan step size of 0.02° in 2θ. The PXRD patterns (Fig. S1) indicate that when **1** and **1**@Tb$(NO_3)_3$ were respectively immersed in benzaldehyde and DMF for three days, the structure of **1** retains unchanged. Thermogravimetric analyses (TGA) were carried out using a HCT-2 thermal analyzer under air from room temperature to 800 °C with a heating rate of 10 °C·min^{-1}. Infrared (IR) spectra were measured on a Bruker Tensor37 spectrophotometer using the KBr pellets technique. Fluorescence spectra were collected on an FL7000 fluorescence spectrophotometer (Japan Hitachi company) at room temperature in same conditions.

Synthesis of complexes

Preparation of [Zn(3,3′-dpdc)bpp] (1): A mixture of $Zn(OAc)_2$ (0.0185 g, 0.10 mmol), 3,3′-H_2dpdc (0.0242 g, 0.10 mmol), bpp (0.0198 g, 0.10 mmol), 1 mol/L NaOH (1.0 ml) and distilled water (10 ml) was sealed in a Teflon-lined reactor and heated at 120°C for 3 days. Yield: 56% based on Zn. Anal. Calc. for $C_{27}H_{22}ZnN_2O_4$ (503.84): C, 64.35; H, 4.37; N, 5.56%. Found: C, 64.42; H, 4.15; N, 5.34%. Selected IR (KBr pellet, ν / cm^{-1}): 3434(m), 1619(s), 1594(s), 1571(s), 1414(s), 1385(s), 1265(m), 1225(m), 1071(w), 1036(w), 908(w), 846(w), 806(w), 758(s), 694(s), 622(w), 462(w), 437(w).

Preparation of [Cd(3,3′-dpdc)bpp] (2): A mixture of $CdSO_4$·8/3H_2O (0.0256 g, 0.10 mmol), 3,3′-H_2dpdc (0.0243 g, 0.10 mmol), bpp (0.0199 g, 0.10 mmol), 1 mol/L NaOH (1.0 ml) and distilled water (10 ml) was sealed in a Teflon-lined reactor and heated at 140°C for 3 days. Yield: 61% based on Cd. Anal. Calc. for $C_{27}H_{22}CdN_2O_4$ (550.87): C, 58.82; H, 3.99; N, 5.08%. Found: C, 58.77; H, 4.01; N, 4.78%. Selected IR (KBr pellet, ν / cm^{-1}): 3436(m), 1613(s), 1585(w), 1549(vs), 1411(s), 1385(vs), 1261(w), 1224(m), 1071(w), 1017(w), 921(w), 858(w), 808(w), 763(s), 688(s), 515(w), 425(w).

Preparation of [Cu(3,3′-dpdc)$(bpp)_{0.5}$] (**3**): A mixture of $CuSO_4$·5H_2O (0.0501 g, 0.20 mmol), 3,3′-H_2dpdc (0.0483 g, 0.20 mmol), bpp

Table 1 crystallographic data of the complexes **1**-**3**

Complex	**1**	**2**	**3**
Empirical formula	$C_{27}H_{22}ZnN_2O_4$	$C_{27}H_{22}CdN_2O_4$	$C_{41}H_{30}Cu_2N_2O_8$
Formula weight	502.83	550.87	805.75
Temperature / K	296(2)	296(2)	296(2)
Wavelength / Å	0.71073	0.71073	0.71073
Crystal system	orthorhombic	orthorhombic	monoclinic
Space group	Pbca	Fddd	$P2_1/c$
a / Å	17.7194(7)	10.5042(13)	10.0555(15)
b / Å	11.7120(5)	43.810(4)	18.049(3)
c / Å	23.0697(9)	43.810(4)	10.8042(17)
β / (°)	90	90	107.127(5)
V / Å^3	4787.6(3)	20161(4)	1873.9(5)
Z	8	32	2
D_{calcd} (g cm^{-3})	1.395	1.452	1.428
Absorption coefficient(mm^{-1})	1.062	0.901	1.190
F (000)	2072	8896	824
Crystal size (mm^3)	0.41 x 0.17 x 0.08	0.35x 0.18 x 0.06	0.23 x 0.10 x 0.07
θ range for data collection (°)	3.02 ~25.10	2.94 ~ 25.10	3.00 ~25.10
Limiting indices	-21<=h<=20 -13<=k<=13 -27<=l<=27	-11<=h<=12 -52<=k<=52 -52<=l<=52	-11<=h<=12 -21<=k<=21 -12<=l<=12
Reflections collected/ unique	60458 / 4255 [R(int) = 0.0988]	64411 / 4500 [R(int) = 0.0953]	32865 / 3315 [R(int) = 0.0762]
Data/restraints/parameters	4255 / 0 / 307	4500 / 188 / 381	3315 / 258 / 348
Goodness-of-fit on F^2	1.017	1.067	1.017
R_1, wR_2 [I>2σ(I)]	R1 = 0.0499, wR2 = 0.1199	R1 = 0.0422, wR2 = 0.0941	R1 = 0.0371, wR2 = 0.0801
R_1, wR_2 [all data]	R1 = 0.0811, wR2 = 0.1412	R1 = 0.0663, wR2 = 0.1101	R1 = 0.0595, wR2 = 0.0888
Largest diff. peak and hole (e$^-$Å^{-3})	0.739 and -0.375	0.644 and -0.402	0.402 and -0.278
CCDC No.	1402459	1402456	1402458

(0.0199 g, 0.10 mmol), 1 mol/L NaOH(4.0 ml) and distilled water (10 ml) was sealed in a Teflon-lined reactor and heated at 160°C for 3 days. Yield: 59% based on Cu. Anal. Calc. for $C_{41}H_{30}Cu_2N_2O_8$ (805.75): C, 61.12; H, 3.75; N, 3.48%. Found: C, 60.84; H, 3.68; N, 3.36 %. Selected IR (KBr pellet, v / cm^{-1}): 3431(m), 1633(s), 1596(m), 1572(s), 1414(vs), 1386(vs), 1269(w), 1220(w), 1175(w), 1079(w), 1054(w), 1021(w), 904(w), 850(w), 813(w), 758(s), 699(s), 622(w), 491(m).

$ZnSO_4 \cdot 7H_2O$ was used instead of $Zn(OAc)_2$, complex **1** was also obtained. In other words, all sulfate salts ($ZnSO_4 \cdot 7H_2O$, $CdSO_4 \cdot 8/3H_2O$ and $CuSO_4 \cdot 5H_2O$) were used, complexes **1**-**3** were obtained. In the three complexes, the anions are not coordinated to the metal centers, the anion of the metal salts have no effect on the products.

X-ray Crystallography Study

The x-ray single crystal data of complexes **1**-**3** collections were performed on a Bruker D8 QUEST CCD diffractometer equipped with a graphite monochromatized MoKα radiation (λ=0.71073 Å) at 296(2)K. Semi-empirical absorption corrections were applied. The structures were solved by direct methods and refined by full-matrix least-squares method on F^2 with the SHELXS 97 and SHELXL-97 programs[9]. All non-hydrogen atoms in the complexes were refined anisotropically. The hydrogen atomswere generated geometrically and treated by amixture of independent and constrained refinement. The crystallographic data of the complexes **1**-**3** are listed in Table 1, while the selected bond lengths and angles are given in Supporting Information Table S1.

Description of the crystal structures

Structure of [Zn(3,3′-dpdc)bpp] (**1**). Complex **1** crystallizes in orthorhombic space group Pbca and features an unusual 3D network structure (Fig. 1). The asymmetric unit of **1** contains one Zn(II) ion, one 3,3′-dpdc ligand, and one bpp ligand (Fig. 1a). Zn(II) ion is four-coordinated by two oxygen atoms (O1A and O4) from two 3,3′-dpdc ligands (d(Zn-O)= 1.905(4) and 1.956 (2) Å) and two nitrogen atoms (N1B and N2) from two bpp ligands (d(Zn-N)= 1.999 (6) and 2.070 (3) Å). The ZnO_2N_2 is in distorted tetrahedral geometry with the corresponding angles in the range of 95.1–125.3°, deviating from 109.5°, the angle for perfect tetrahedrons. All bpp ligands exhibit the TT conformation with the dihedral angles of the pyridyl ring planes at 32.9° and the N…N distance of 10.202(3) Å. The bpp molecule acts as a bis(monodentate) bridging ligand that links two different Zn(II) ions with the Zn…Zn distance at 13.812(2) Å (Fig. 1b), while the 3,3′-dpdc ligand adopts a bis(monodentate) coordination mode (Scheme 1a) and links two Zn(II) ions with the Zn…Zn distance at 12.706(1) Å. The ZnO_2N_2 moieties as four-connected (4-c) nodes are further linked by 3,3′-dpdc ligands and bpp ligands to form a 3D framework (Fig. 1c). Interestingly, there are three types of helices in the 3D structure. The Zn-3,3′-dpdc left (L) and right (R) -handed helix has a repeat unit consisting of two Zn(II) centers and two 3,3′-dpdc ligands with a pitch of 17.719 Å (Fig. 1d). The Zn-3,3′-dpdc-bpp (L) and (R) -handed helix is constructed by the alternate Zn(II), bpp and 3,3′-dpdc ligands, and has a repeat unit consisting of four Zn(II) centers, two 3,3′-dpdc ligands and two bpp ligands with a pitch of 23.424 Å (Fig. 1e). However, the other

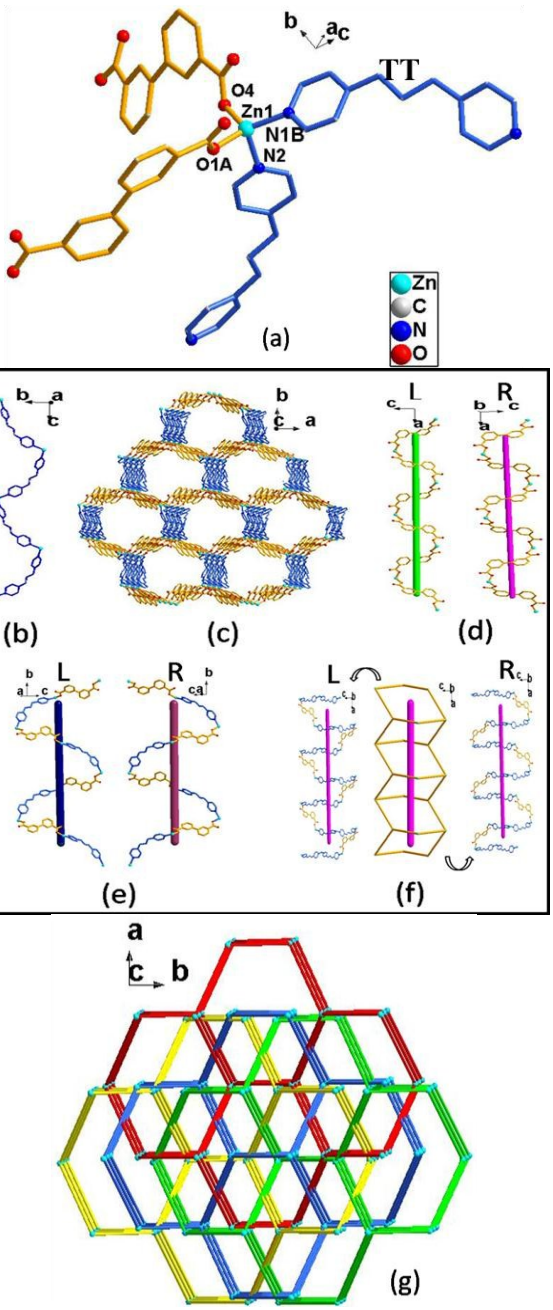

Fig. 1The structure of **1** (a) the coordination environment of the Zn(II) ion, (b) the Zn-bpp chain, (c) 3D framework, (d) Zn-3,3′-dpdc (L) and (R)-handed helix, (e) Zn-3,3′-dpdc-bpp (L) and (R) -handed helix, (f) Zn-3,3′-dpdc-bpp double helical chain, (g) a four fold-interpenetrating net with the topology of 6^6. Symmetry code: A: -0.5 + x, 2.5 + y, 1 - z. B: x, 1.5 - y, 0.5+z.

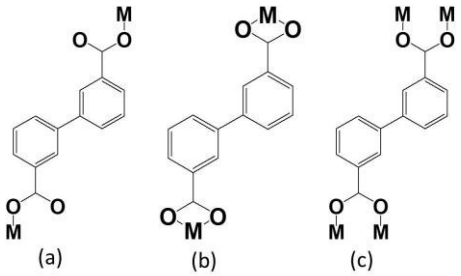

Scheme 1 The coordination modes of the 3,3′-dpdc ligand.

Zn-3,3′-dpdc-bpp double helical strand consists of six Zn(II) centers, two 3,3′-dpdc ligands and four bpp ligands with a pitch of 17.719 Å (Fig. 1f). These chains form a 3D structure with large rhombic channels. It is noteworthy that four identical nets interpenetrate in a parallel fashion and build a four fold-interpenetrating architecture (Fig. 1g). Analysis with TOPOS software[10] revealed that the overall structure is a four fold-interpenetrating 3D diamondoid framework with 4-c Zn(II) nodes and topology with the Schläfli point symbol 6^6. Nevertheless, MOFs with 6^6 topologies are rare[11]. Though such nets contain large channels, the channels are mainly filled with other interpenetrated nets, leaving only small cavities. A calculation with PLATON[12] showed that the total cavity volume was 166.5 Å^3 (3.5% of the unit cell volume).

Structure of [Cd(3,3′-dpdc)bpp] (**2**). Complex **2** crystallizes in orthorhombic space group Fddd and has an unusual 3D network structure (Fig. 2), which is completely different from that of **1**. Its asymmetric unit contains one Cd(II) ion, one 3,3′-dpdc and one bpp ligand (Fig. 2a). Cd(II) center is in a {CdO_4N_2} distorted octahedral coordination geometry with four oxygen atoms (O1, O2, O3, and O4A) from three 3,3′-dpdc ligands (d(Cd-O)= 2.450(3), 2.330(3), 2.267(3), and 2.273(3) Å) and two nitrogen atoms (N1 and N2B) from two bpp ligands (d(Cd-N)= 2.355 (5) and 2.351 (6) Å). These N atoms occupy the axial positions with the N–Cd–N bond angle at 179.4°. The bpp ligand adopts the TG conformation with the dihedral angle between two pyridine rings at 27.8° and the N…N distance at 9.328(9) Å. The bpp as bis-monodentate links two different Cd(II) ions that are 13.536(1) Å apart. The 3,3′-dpdc ligands adopt bi(bidentate-chelating) and bi(bidentate-bridging) coordination modes (Scheme 1b and 1c) and bind two Cd(II) and four Cd(II) ions, respectively. The two closest Cd(II) centers are bridged by two COO groups to form a binuclear secondary building unit (SBU), $Cd_2(COO)_2$ (Fig. 2b), with Cd…Cd distance at 4.062 (2) Å. Each SBU and six nearest SUBs are linked together by four 3,3′-dpdc ligands and four bpp ligands to form an extended 3D network (Fig. 2c). With SBU as the node for this framework, the structure of **2** can be described as a (6-c) net with a $\{3^6.4^{12}.5^4.6^6\}$ topology. An interesting feature of this network is the presence of two types of helices along the a axis. The Cd-3,3′-dpdc-bpp two-flexural (L and R)-handed helix is formed by bpp and 3,3′-dpdc ligands bridging the SUBs ($Cd_2(COO)_2$) (Fig. 2d), and has a repeat unit consisting of two SUBs, one bpp ligand and one 3,3′-dpdc ligand with a pitch of 21.008 Å. The four-flexural (L) and (R) -handed helixis constructed with 3,3′-dpdc ligands bridging the Cd(II) ions (Fig. 2e), and has a repeat unit consisting of four Cd(II) centers and four 3,3′-dpdc ligands with a pitch of 42.017 Å. The final 3D net is an assembly of these helical subunits. A calculation by PLATON[12] showed a total void volume of 1084.9 Å^3 (5.4% of the unit cell volume).

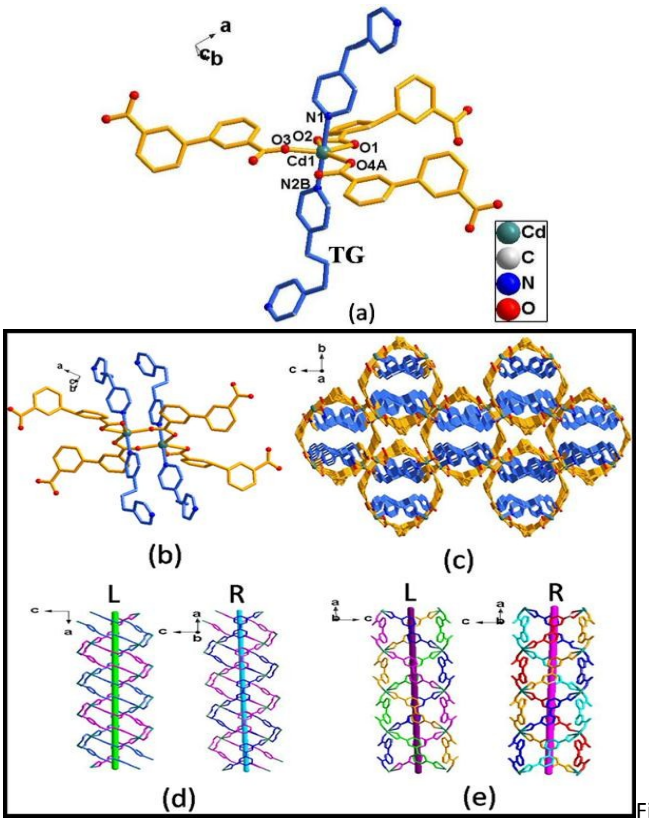

Fig. 2 The structure of **2** (a) the coordination environment of the Cd(II) ion, (b) binuclear secondary building unit (SBU), (c)3D framework, (d) two-flexural (L) and (R)-handed helix, (e) four-flexural (L) and (R)-handed helix. Symmetry code: A: 3.5 - x, - y, -0.5 - z. B: -0.75 + x, - y, 0.25 + z.

Structure of [Cu(3,3′-dpdc)$(bpp)_{0.5}$] (**3**). Complex **3** crystallizes in monoclinic space group $P2_1/c$ group and features an unusual 3D network structure (Fig. 3). Its asymmetric unit consists of one Cu(II) ion, one 3,3′-dpdc ligand and one and half bpp ligands (Fig. 3a). Cu(II) ion is coordinated to four oxygen atoms (O1, O2A, O3B and O4C) from four 3,3′-dpdc ligands (d(Cu-O)= 1.974(3), 1.960(1), 1.962(1) and 1.968(8) Å) and one nitrogen atom (N1) from bpp ligand (d(Cu-N)= 2.141(9) Å). Cu(II) center is in a {CuO_4N_1} square-pyramidal coordination geometry. The apical position is occupied by N1 atom while Cu(1)-N(1) bond (2.141(9) Å) is significantly longer than bonds in basal plane, since there is Jahn-Teller distortion. The bis-monodentate bpp ligand assumes a TT conformation (0.000(6)° torsion with d(N…N) = 9.917(5) Å) and bridges two Cu(II) ions with the Cu…Cu length of 14.152(9) Å. The 3,3′-dpdc ligand adopts bi(bidentate-bridging) coordination mode (Scheme 1c) and links four different Cu(II) ions with the Cu…Cu distance at 13.532(3) Å. The closest two Cu(II) ions are linked by four COO groups to form a centrosymmetric binuclear unit $Cu_2(COO)_4$ with a Cu…Cu distance at 2.645 Å, an unit defined as a SBU (Fig. 3b). This SBU is linked by four 3,3′-dpdc ligands and two bpp ligands which bridge six adjacent SUBs, extending into a 3D framework structure (Fig. 3c). Interestingly, the Cu-3,3′-dpdc and Cu-bpp-3,3′-dpdc helical chains are found. The Cu-3,3′-dpdc (L) and (R) - handed helical chain is formed by 3,3′-dpdc ligands bridging adjacent Cu(II) ions (Fig. 3d), and contain a repeat unit consisting of two Cu(II) centers and two 3,3′-dpdc ligands with a pitch of 18.049 Å. The Cu-bpp-3,3′-dpdc double strand helical chain has a repeat unit consisting of four Cu(II) centers, two 3,3′-dpdc ligands and two bpp ligands with a pitch of 18.049 Å (Fig. 3e). These helical chains further form a 3D structure with large square channels. Notably, those three identical 3D frameworks interpenetrate in a parallel fashion, leading to a three fold-interpenetrating architecture with a $\{3^{12}.4^{28}.5^5\}$ topology (Fig. 3f). Upon interpenetration, the framework only has porous void volume of 132.7 Å^3 (7.1% of the unit cell volume) based on the PLATON calculation [12].

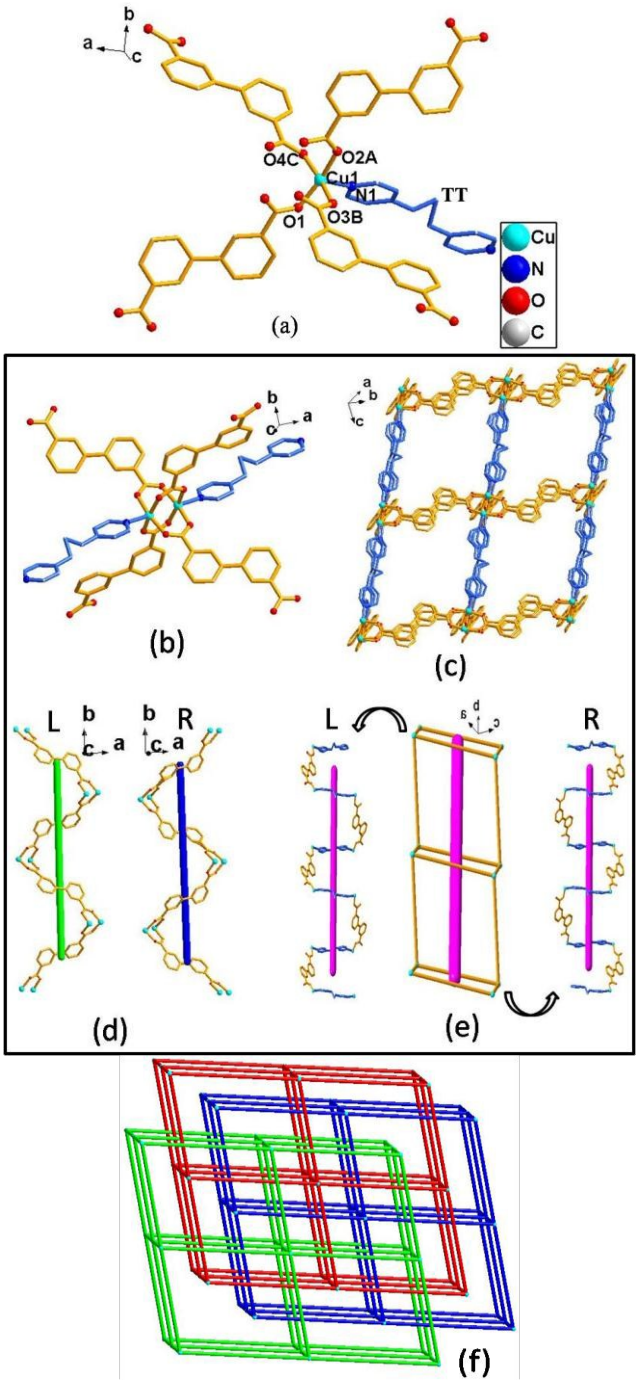

Fig. 3 The structure of **3** (a) the coordination environment of the Cu(II) ion, (b) the binuclear unit (SUB), (c) 3D framework, (d) Cu-3,3′-dpdc(L) and (R) -handed helical chains, (e) Cu-bpp-3,3′-dpdc (L) and (R)-handed helical chains, (f) a three fold-interpenetrating net with$\{3^{12}.4^{28}.5^{5}\}$ topology. Symmetry code: A: 2 - x, - y, 2 - z. B: -1 + x, -0.5 - y,-0.5 - z; C: 3 - x, 0.5 + y, 2.5 - z.

The structural features of the three coordination architectures are direct results of the coordination geometry modes of metal centers and the conformations of ligands. The three MOFs carry tetrahedral (Zn(II)), octahedral (Cd(II)) and square-pyramidal (Cu(II)) metal centers as nodes, respectively, with 3,3′-dpdc and bpp as linker ligands. The metal coordination geometries determine the bridging mode of the carboxylate ligand and the conformation of flexible N-ligand, leading to a variety of structural motifs in the frameworks **1**-**3**. In other words, the metal center plays a very important role in tuning the structure of each specific network because metal-cluster nodes generally have large surface and can accommodate the steric demands of organic ligands more readily. The thermal stabilities of all the complexes were explored by means of thermogravimetric analyses (TGA) in the temperature range room temperature–800°C. TGA analysis indicates that the frameworks are stable up to 282-306 °C and completely decompose at 404-484°C (Fig. S2).

Photoluminescence properties

The solid-state luminescence spectra of the complexes and free ligands were taken at room temperature (Fig. 4). The emission spectra show broad bands at 385 nm for 3,3′-dpdc (λ_{ex} = 278 nm) and at 408 with shoulder peaks at 386 and 431 nm for bpp (λ_{ex} = 361 nm). The emission spectra of the complexes show broad bands at 384 nm for **1** and 425 nm for **2** with the excitation wavelengths at 330 nm for **1** and 321 nm for **2**. These emission maxima match closely with those of the free 3,3′-dpdc or bpp ligands. The Zn(II)/Cd(II) ions have a d^{10} configuration, the metal ions do not show *d–d* electronic transitions. Therefore, the emissions of **1** and **2**

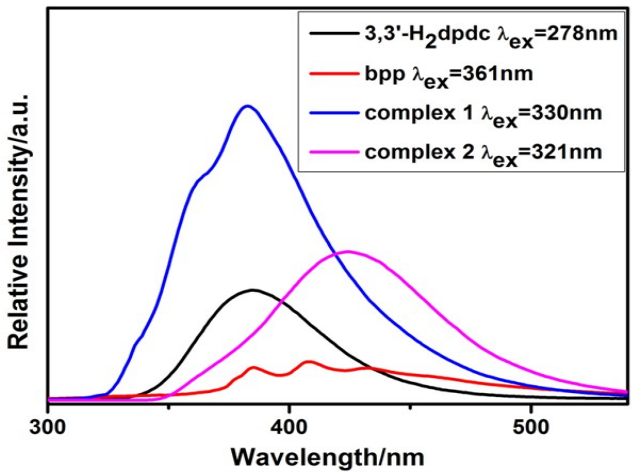

Fig. 4 The solid state emission spectra of complexes **1**-**2** and the free ligands.

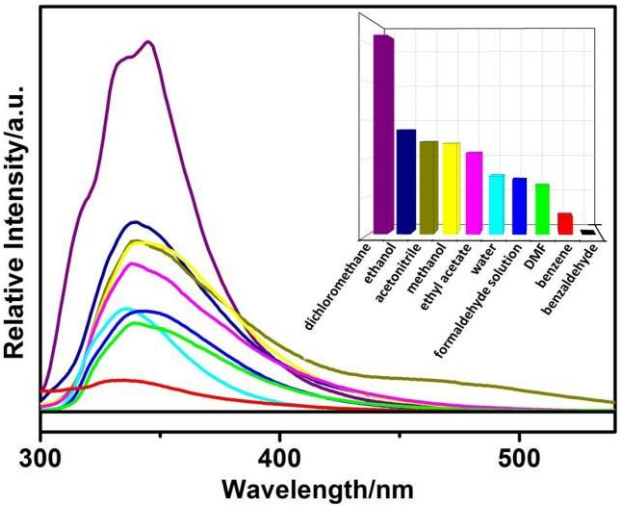

Fig. 5 Emission spectra of **1** dispersed in different solvents (λ_{ex} = 283nm).

should come from ligand-centered π^*-π. The enhancement of fluorescence intensities for **1** and **2** is closely associated with the metal ions and the ligand coordinated around them.[13] For **3**, no emissions observed. Herein complex **1** is selected for further investigation on the luminescence property and potential detection application on small organic molecules. Complex **1** was immersed in several solvents, such as dichloromethane, ethanol, acetonitrile, methanol, ethyl acetate, water, formaldehyde solution, N,N-dimethylformamide (DMF), benzene, and benzaldehyde, to form suspensions. Their luminescent spectra were measured. Fig. 5 shows the emission spectra of **1** dispersed in different solvents. It's clear that the luminescence properties of the suspensions highly depended on the solvents. The maximum emission bands of the suspensions centered at 377- 401 nm exhibit minor shifts (7-17 nm), compared with that of **1** in the solid state. The maximum emission bands of the suspensions are shifted by 9-49 nm as compared to that of various solvents (Fig. S3). The luminescence intensity is dramatically changed. The phenomena might be due to the solvent effect.[2a-f] Dichloromethaneis proved to be the strongest enhancer, while benzaldehyde is the most effective quencher. Notably, the benzaldehyde can quench the fluorescence of the Zn-MOF complex completely. Such solvent-dependent luminescence would be very useful in detecting pollution molecule benzaldehyde. To explore the sensitivity of **1** as benzaldehyde probe, a series of suspensions of **1** were prepared in ethanol with benzaldehyde at different concentrations (0, 50, 100, 200, 300, 400, 500 and 600 ppm) and the resulted suspensions were measured for their emissive responses. As shown in Fig. 6a, the luminescent intensity of the suspensions significantly decreases with an increasing in benzaldehyde concentration. The luminescent intensity of the suspension decreases by 30% at the addition 50 ppm of benzaldehyde, which would allow us to detect small amounts of benzaldehyde in the solvents. With the presence of 600 ppm benzaldehyde, the emission intensity is cut by nearly 100%. The data indicates that compound **1** can serve as a fluorescence probe to detect the benzaldehyde at ppm level. Nevertheless, to the best of our knowledge, reports about MOFs as luminescent probes for sensing benzaldehyde are rare. [2a] In addition, the quenching effect of benzaldehyde in dichloromethane is also investigated (Fig. 6b). In order to understand the sensing mechanism for benzaldehyde, the emission of **1** dispersed in ethanol containing toluene, nitrobenzene

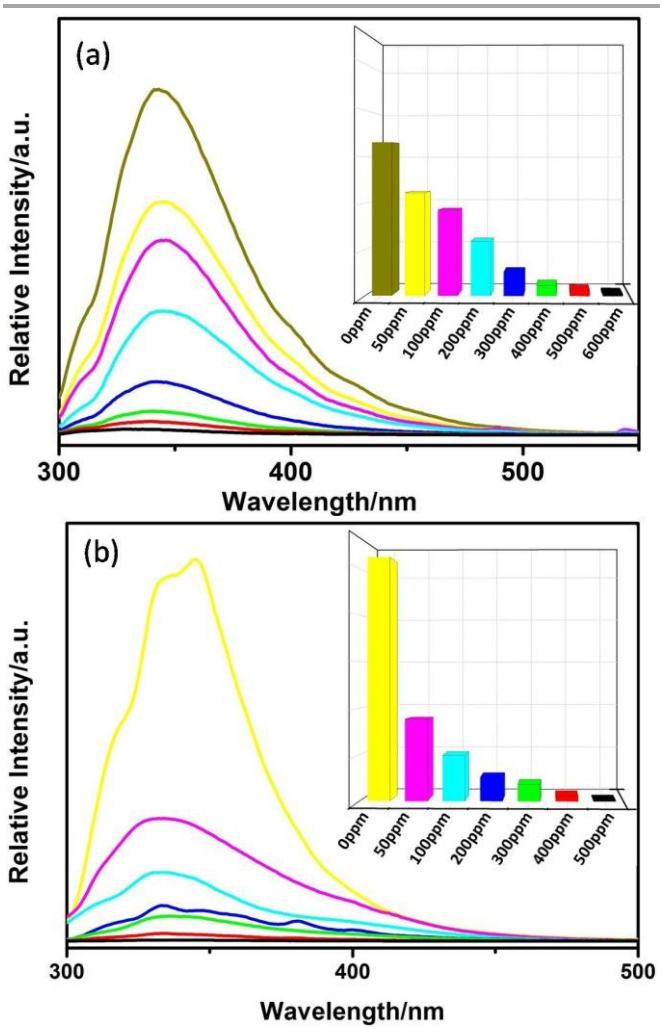

Fig. 6 Emission spectra of **1** dispersed in ethanol (a) and dichloromethane (b) with different concentrations of benzaldehyde (λ_{ex} = 283nm).

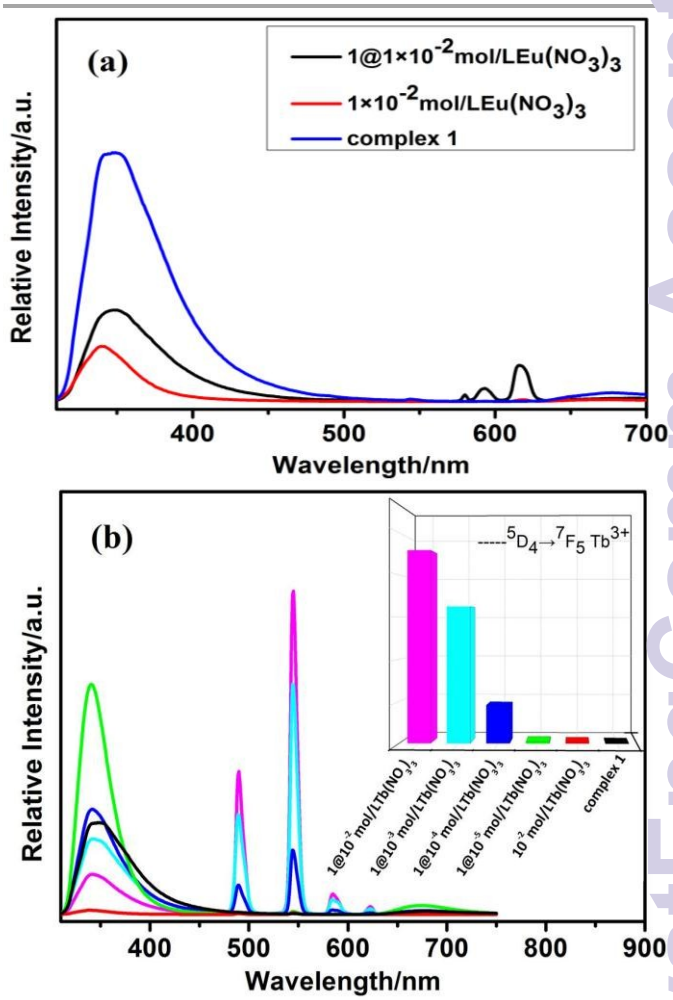

Fig. 7 Emission spectra of complex **1,** $Ln(NO_3)_3$ and **1**@$Ln(NO_3)_3$ aqueous solution (Ln=Eu(a), Tb(b)) (λ_{ex}=288*nm).* Inset, $^5D_4 \rightarrow {}^7F_5$ emission intensities.

and o,m,p-xylenes separately was taken at room temperature. The emission spectra show the different luminescence intensity (Fig. S4). However, nitrobenzene and benzaldehyde are the most effective quenchers, which can be related to the donor–acceptor electron-transfer mechanism.[2a, b, h] Here, the aldehyde/ nitro groups have electron-withdrawing property, the benzaldehyde/nitrobenzene are the electron acceptors. Thus, upon excitation, the electron transfers from the electron-donating framework **1** to the benzaldehyde/nitrobenzene molecules, resulting in the luminescence quenching. The obvious quenching phenomenon for nitrobenzene indicates that **1** is also promising fluorescent probe for detecting nitrobenzene.

As a matter of fact, MOFs have advantages in detecting lanthanide cations, too. Here, we explored the possibility of using **1** to sensitize lanthanide (Ln) ions. Complex **1** was immersed in aqueous $Ln(NO_3)_3$ (Ln = Eu, Tb) solutions with Ln concentration of 10^{-2} mol/L, yielding **1**@$Ln(NO_3)_3$. The

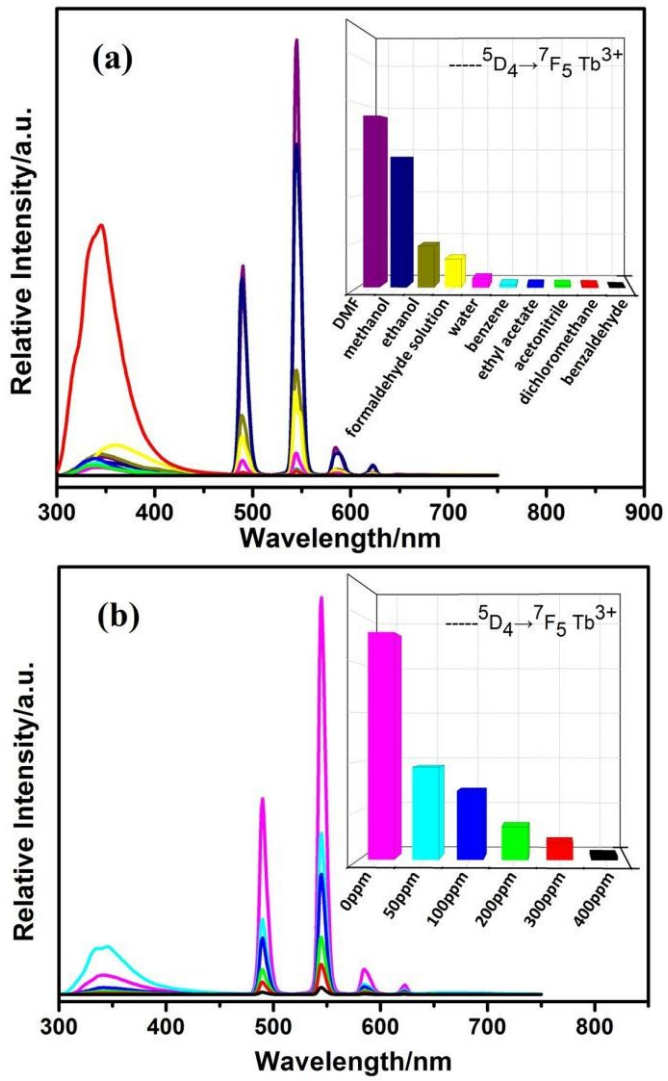

Fig. 8 Emission spectra of **1**@$Tb(NO_3)_3$ dispersed in different solvents (a) and **1**@$Tb(NO_3)_3$ dispersed in DMF with different concentrations of benzaldehyde (b) Inset, $^5D_4 \rightarrow {}^7F_5$ emission intensities (λ_{ex} =288 nm).

fluorescence of **1**@$Eu(NO_3)_3$ indicates very weak emissions of Eu(III) at 579, 592 and 617 nm, corresponding to the $^5D_0 \rightarrow {}^7F_J$ (J = 0–2) transitions of Eu(III), respectively (Fig. 7a). However, the **1**@$Tb(NO_3)_3$ shows strong characteristic emission of Tb(III) (Fig 7b). The emission bands at 490, 544, 586 and 622 nm corresponding to the $^5D_4 \rightarrow {}^7F_J$ (J = 6–3) transitions of Tb(III), respectively. The most intense transition is $^5D_4 \rightarrow {}^7F_5$ (at 544 nm), which is responsible for the green emission. When the Tb(III) concentration increased from 10^{-5} to 10^{-2}mol/L, the emission intensity of Tb(III) from the **1**@$Tb(NO_3)_3$ is gradually enhanced, while the emission intensity at 344 nm from the ligands is gradually reduced. It is well known that the ligands could absorb UV energy and transfer it to Ln(III) ion, leading to f–f emissions of Ln(III). Our results show that the energy of the Zn-MOF framework match well with the excitation energy of the Tb(III) ion, leading to strong characteristic luminescence of the Tb(III). The enhanced luminescence of the **1**@$Tb(NO_3)_3$ suggests high efficiency of the energy transfer within the **1**@$Tb(NO_3)_3$ from the metal bound ligands subunit to the Tb(III) ion. The result confirmed that Zn-MOF acts as an antenna and selectively sensitizes Tb(III) fluorescence. The mechanism for such enhancing fluorescence effect remains unclear.[2i] It is clear that the efficiency is high for the energy transformation from ligands to Tb(III) ion through the binding interaction of the Zn-MOF in $Tb(NO_3)_3 \cdot H_2O$. We believe that Tb(III) might be diffused into the microporous of **1** or attached to the surface of **1** via hydrogen-bond interactions. Based on the above research results and analysis, Zn–MOF is good chromophore for sensing Tb(III) fluorescence. To examine the potential of the **1**@$Tb(NO_3)_3$ for detecting organic small molecules, the **1**@$Tb(NO_3)_3$ (10^{-2} mol/L $Tb(NO_3)_3$) was immersed in above organic solvents (dichloromethane, ethanol, acetonitrile, methanol, ethyl acetate, water, formaldehyde solution, DMF, benzene, benzaldehyde) to form the suspensions. The fluorescence spectra (Fig. 8a) of these suspensions show the characteristic Tb(III) emission from the **1**@$Tb(NO_3)_3$. The emission bands show no shift while the emission intensity is different with different solvents. It is believed that differences in the vibronic strength for different solvent molecules led to the changes in luminescence intensity. In this case, the luminescence increases when the compound was immersed in DMF, but decreases when immersed in benzaldehyde. Similarly, with the presence of benzaldehyde, **1**@$Tb(NO_3)_3$ luminescent intensity is proportionally lowered with the change of benzaldehyde concentration (Fig. 8b). With the addition of 50 ppm benzaldehyde, the emission intensity (at 545 nm) of Tb(III) from **1**@$Tb(NO_3)_3$ decreases by approximately 60%, which is about twice as strong as that (30%) of **1** without Tb(III) ion under the addition of same concentration of benzaldehyde (50 ppm) in ethanol. The addition of benzaldehyde into the suspension of **1**@$Tb(NO_3)_3$ could lead to a significant drop of the luminescent intensity. While with the addition of 300 ppm benzaldehyde, the emission intensity is quenched by nearly 93%. Our results show that addition of Tb(III) into the Zn-MOF can enhance the sensing ability for benzaldehyde.

Conclusions

Three unique MOFs containing transition metal Zn(II), Cd(II) and Cu(II) and semi-rigid carboxylic acid and flexible N- ligand were synthesized. The new MOFs have 3D microporous and/or interpenetrating structures. Compound **1** shows solvent-dependent emissions. Interestingly, compound **1** can be used to detect benzaldehyde with relatively high selectivity and sensitivity in 10 kinds of different organic solvents. Furthermore, compound **1** is also as a luminescent probe for Tb(III) ion. In particular, the combination of Zn-MOF and luminescence Tb(III) ion shows high sensitivity for sensing benzaldehyde. Therefore, MOFs are promising luminescent probes for organic small molecule detection.

Acknowledgements

The authors are grateful to the National Natural Science Foundation of China (21471104), the Science and Technology Program, Beijing Municipal Education Commission (KM201510028006) and Scientific Research Base Development Program of the Beijing Municipal Commission of Education. We also thank Dr. Xue-Bin Deng from Beijing Normal University for helpful work and discussions.

Notes and references

1 (a) J. R. Long and O. M. Yaghi, *Chem. Soc. Rev.*, 2009, **38**, 1213; (b) E. D. Bloch, W. L. Queen, R. Krishna, J. M. Zadrozny, C. M. Brown and J. R. Long, *Science*, 2012, **335**, 1606; (c) H.X. Deng, S. Grunder, K. E. Cordova, C. Valente, H. Furukawa, M. Hmadeh, F. Gándara, A. C. Whalley, Z. Liu, S. Asahina, H. Kazumori, M. O'Keeffe, O. Terasaki, J. F. Stoddart and O. M. Yaghi, *Science*, 2012, **336**, 1018; (d) M. P. Suh, H. J. Park, T. K. Prasad and D. Lim, *Chem. Rev.*, 2012, **112**, 782; (e) L. Gao, C. Y. V. Li, and K.Y. Chan, *Chem. Mater.*, 2015, **27**, 3601; (f) D. Maspoch, D. Ruiz-Molinaa and J. Veciana，*Chem. Soc. Rev.*, 2007, **36**, 770; (g) B. V. Harbuzaru, A. Corma, F. Rey, P. Atienzar and J. L. Jord, *Angew. Chem. Int. Ed.*, 2008, **47**, 1080; (h) L. E. Kreno, K. Leong, O. K. Farha, M. Allendorf, R. P. V. Duyne, and J. T. Hupp, Chem. Rev. 2012, **112**, 1105.

2 (a) B. B. Shi, Y. H. Zhong, L. L. Guo and G. Li, *Dalton Trans.*, 2015, **44**, 4362; (b) D. Singh and C. M. Nagaraja ,*Dalton Trans.*, 2014, **43**, 17912; (c) S. N. Zhao, X. Z. Song, M. Zhu, X. Meng, L. L. Wu, J. Feng, S. Y. Song, and H. J. Zhang, *Chem. Eur. J.*, 2015, **21**, 1; (d) Z. Y. Guo, X. Z. Song, H. P. Lei, H. L. Wang, S. Q. Su, H. Xu, G. D. Qian, H. J. Zhang and B. L, Chen. *Chem. Commun.*, 2015, **51**, 376; (e) A. J. Lan, K. H. Li, H. H. Wu, D. H. Olson, T. J. Emge, W. Ki, M. C. Hong, and J. Li, *Angew. Chem. Int. Ed.*, 2009, **48**, 2334; (f) Y. F. Yue, A. J. Binder, R. J. Song, Y. J. Cui, J. H. Chen, D. K. Hensleyd and S. Dai. *Dalton Trans.*, 2014, **43**, 17893; (g) F. H. Liu, C. Qin, Y. Ding, H. Wu, K. Z. Shao andZ. M.Su,*Dalton Trans.*, 2015, **44**, 1754;(h)Y. N. Wang, P. Zhang, J. H. Yu and J. Q. Xu,*Dalton Trans.*, 2015, 44, 1655. (i) Y. F. Gao, X. Q. Zhang, W. Sun and Z. L. Liu,*Dalton Trans.*, 2015, **44**, 1845; (j) H. L. Tan, Q. Li, C. J. Ma, Y. H. Song, F. G. Xu, S. H. Chen and L. Wang. *Biosensors and Bioelectronics*, 2015, **63**, 566; (k) F. Luo and S. R. Batten, *Dalton Trans.*, 2010, **39**, 4485; (l) X. Y. Xu and B. Yan, *ACS Appl. Mater. Interfaces*,2015, **7**, 721; (m) B. Zhao, X. Y. Chen, P. Cheng, D. Z. Liao, S.P. Yan and Z. H. Jiang, *J. Am. Chem. Soc.*,2004, **126**, 15394;

3 (a) M. D. Allendorf,C. A. Bauer,R. K. Bhaktaaand R. J. T. Houk, *Chem. Soc. Rev.*, 2009, **38**, 1330; (b) S. R. Batten, *CrystEngComm*, 2001, **18**, 1; (c) V. A. Blatov, L. Carlucci, G. Ciani and D. M. Proserpio, *CrystEngComm*, 2004, **6**, 377.

4 C. Janiak, *Dalton Trans.*, 2003, 2781.

5 (a) M.X. Zheng, X. J. Gao, C. L. Zhang, L. Qin and H. G. Zheng, *Dalton Trans.*, 2015, **44**, 4751; (b) H. Wu, W. J. Sun, T. Shi, X. Z. Liao, W. J. Zhao and X. W. Yang, *CrystEngComm*, 2014, **16**, 11088; (c) F, Guo, F. Wang, H. Yang, X. L. Zhang, and J. Zhang, *Inorg. Chem.*, 2012, **51**, 9677; (d) H. Erer, O. Z. Yeşilel and M Arıcı, *Cryst. Growth Des.*, 2015, **15**, 3201.

6 (a) D. Singh and C. M. Nagaraja, *Cryst. Growth Des.*, 2015, **15** 3356;(b) M. Arıcı, O. Z. Yeşilel, and M. Tas, *Cryst. Growth Des.*, 2015, **15**, 3024; (c) Z. X. Zhao, Y. W. Li, S. J. Liu, L. F. Wang, Z. Chang, J. Xu and Y. H. Zhang,*CrystEngComm*, 2015, **17**, 4301; (d) L. Yang, C. Qin, B. Q. Song, X. Li, C. G. Wang and Z. M. Su, *CrystEngComm*, 2015, 17, 4517.

7 (a) L. Carlucci, G.Ciani, D. M. Proserpio and S.Rizzato,*CrystEngComm*, 2002, 4, 121; (b)Y. E Cha, X. Li, X Ma, C. Q. Wan, X. B. Deng and L. P. Jin, *CrystEngComm*, 2012, **14**, 5322; (c) P. Lama, R. K. Das, V. J. Smith and L. J. Barbou *Chem. Commun.*, 2014, **50**, 6464; (d) M.L. Zhang, D.S. Li, J.J. Wang, F. Fu, M. Du, K. Zou and X.M. Gao, *Dalton Trans.*, 20 5355; (e) N. Y. Li, Y. Ge, T. Wang, S. J. Wang, X. Y. Ji and D. Liu, *CrystEngComm*, 2014, **16**, 2168; (f) Y. L. Wang, J. H. Fu, Y. J Jiang, Y. Fu, W. L. Xiong and Q. Y. Liu, *CrystEngComm*, 2012, **14**, 7245; (g) F. Yang, B.Y. Li, W. Xu, G.H. Li, Q. Zhou, J. Hua, Z. Shi and S.H. Feng, *Inorg. Chem.*, 2012, **51**, 6813;(h) Y.Q Zheng, J. Zhang and J.Y. Liu, *CrystEngComm*, 2010, **12**, 2740; (i) G. X. Liu, Y. Q. Huang, Q. Chu, T. Okamura, W. Y. Sun, H Liang and N. Ueyama, *Cryst. Growth Des.*, 2008, **8**, 3233.

8 (a)B. Liu, J. T. Shi, K. F. Yue, D. S. Li, and Y. Y. Wang, *Cryst. Growth Des.*, 2014, **14**, 2003; (b) C. Y. Niu, X. F. Zheng, X. S. Wan and C. H. Kou, *Cryst. Growth Des.*, 2011, **11**, 2874; (c) R H. Wang, M. C. Hong, D. Q. Yuan, Y. Q. Sun, L. J. Xu, J. H. Luo, R. Cao and A. S. C. Chan, *Eur. J. Inorg. Chem.*, 2004, **1**, 37; (d) R. H. Wang, L. Han, F. L. Jiang, Y. F. Zhou, D. Q. Yuan, and M. C. Hong, *Cryst. Growth Des.*, 2005, **5**, 129.

9 (a) G. M. Sheldrick, *SHELXS-97*, Program for Crystal Structure Refinement, University of Göttingen (1997); (b) G. M. Sheldrick, *SHELXL-97*, Program for Crystal Structure Solutic University of Göttingen (1997).

10 V. A.Blatov, *IUCrCompCommNewsl*., 2006, **7**, 4

11 (a) M.-H. Bi, G.-H. Li, Y.-H. Zou, Z. Shi and S.-H. Feng, *Inorg. Chem.*, 2007, **46**, 604; (b) G. A. Farnum, A. L. Pochodylo and R. L. LaDuca, *Cryst. Growth Des.*, 2011, **11**, 678.

12 (a)A. L. Spek, *PLATON, A Multipurpose Crystallographic Tool*; Utrecht University: The Netherlands, 2013; (b) A. L. Spek, *J. Appl. Crystallogr.* 2003, **36**, 7.

13 S. Majumder, L. Mandal and S. Mohanta, *Inorg. Chem.*, 2012, **51**, 8739.

Metal(II)–Organic frameworks with 3,3´- diphenyldicarboxylate and 1,3-bis(4-pyridyl)propane as ligands: preparation, crystal structures and luminescent properties

Ting- Ting Fan, Jia- Jia Li, Xiang-Long Qu, Hong- Liang Han, Xia Li*

Department of Chemistry, Capital Normal University, Beijing 100048.

3D frameworks were constructed from Zn(II)/Cd(II)/Cu(II) , 3,3´-diphenyldicarboxylate, and 1,3-bis(4-pyridyl)propane. Zn-framework was used as a fluorescence probe to sense benzaldehyde.